

Quark-gluon vertex model and lattice-QCD data

M. S. Bhagwat and P. C. Tandy

Center for Nuclear Research, Department of Physics, Kent State University, Kent, Ohio 44242, USA

(Received 13 July 2004; published 23 November 2004)

A model for the dressed-quark-gluon vertex, at zero gluon momentum, is formed from a non-perturbative extension of the two Feynman diagrams that contribute at one loop in perturbation theory. The required input is an existing ladder-rainbow model Bethe-Salpeter kernel from an approach based on the Dyson-Schwinger equations; no new parameters are introduced. The model includes an *Ansatz* for the triple-gluon vertex. Two of the three vertex amplitudes from the model provide a pointwise description of the recent quenched-lattice-QCD data. An estimate of the effects of quenching is made.

DOI: 10.1103/PhysRevD.70.094039

PACS numbers: 12.38.Lg, 11.15.-q, 12.38.Gc

I. INTRODUCTION

A great deal of progress in the QCD modeling of hadron physics has been achieved through the use of the ladder-rainbow truncation of the Dyson-Schwinger equations (DSEs). For two recent reviews, see Refs. [1,2]. Apart from one-loop renormalization group improvement, this truncation is built upon a bare quark-gluon vertex. Recent investigations with simple dressed vertex models have indicated that material contributions to a number of observables are possible with a better understanding of the infrared structure of the vertex. These diverse model indications include an enhancement in the quark condensate [3,4], an increase of about 300 MeV in the b_1/h_1 axial-vector meson mass [5], and about 200 MeV of attraction in the ρ/ω vector meson mass.

In the absence of well-constrained nonperturbative models for the vertex, it has often been assumed that a reasonable beginning is the Ball-Chiu [6] or Curtis-Pennington [7] Abelian *Ansatz* times the appropriate color matrix. An example is provided by the recent results from a truncation of the gluon-ghost-quark DSEs where this vertex dressing contributes materially to a reasonable quark condensate value [3]. However, there is no known way to develop a Bethe-Salpeter (BSE) kernel that is dynamically matched to a quark self-energy defined in terms of such a phenomenological dressed vertex in the sense that chiral symmetry is preserved through the axial-vector Ward-Takahashi identity. The latter implementation of chiral symmetry guarantees the Goldstone boson nature of the flavor nonsinglet pseudoscalars independently of model details [8]. There is a known constructive scheme [9] that defines a diagrammatic expansion of the BSE kernel corresponding to any diagrammatic expansion of the quark self-energy such that the axial-vector Ward-Takahashi identity is preserved. For this reason, recent nonperturbative vertex models have employed simple diagrammatic representations [4,5,10,11].

It is only recently that lattice QCD has begun to provide information on the infrared structure of the dressed-quark-gluon vertex [12,13]. In this work we generate a

model dressed vertex, for zero gluon momentum, based on an *Ansatz* for nonperturbative extensions of the only two diagrams that contribute at one-loop order in perturbation theory. An existing ladder-rainbow model kernel is the only required input. We compare to the recent lattice-QCD data without parameter adjustment.

In Sec. II we recall the vertex to one loop in perturbation theory and point out the structure and properties that are used to suggest the *Ansatz* for nonperturbative extension. The nonperturbative extension is described in Sec. III and the results are presented and discussed in Sec. IV.

II. ONE-LOOP PERTURBATIVE VERTEX

We denote the dressed-quark-gluon vertex for gluon momentum k and quark momentum p by $igt^c\Gamma_\sigma(p+k, p)$, where $t^c = \lambda^c/2$ and λ^c is an SU(3) color matrix. Through $\mathcal{O}(g^2)$, i.e., to one loop, the amplitude Γ_σ is given, in terms of Fig. 1, by¹

$$\Gamma_\sigma(p+k, p) = Z_{1F}\gamma_\sigma + \Gamma_\sigma^A(p+k, p) + \Gamma_\sigma^{NA}(p+k, p) + \cdots, \quad (1)$$

with

$$\Gamma_\sigma^A(p+k, p) = -\left(C_F - \frac{C_A}{2}\right) \int_q^\Lambda g^2 D_{\mu\nu}(p-q) \times \gamma_\mu S_0(q+k) \gamma_\sigma S_0(q) \gamma_\nu, \quad (2)$$

and

$$\Gamma_\sigma^{NA}(p+k, p) = -\frac{C_A}{2} \int_q^\Lambda g^2 \gamma_\mu S_0(p-q) \times \gamma_\nu D_{\mu\mu'}(q+k) i\Gamma_{\mu'\nu'\sigma}^{3g}(q+k, q) D_{\nu'\nu}(q), \quad (3)$$

where $\int_q^\Lambda = \int d^4q/(2\pi)^4$ denotes a loop integral regularized in a translationally invariant manner at mass scale Λ . Here $Z_{1F}(\mu^2, \Lambda^2)$ is the vertex renormalization constant to ensure $\Gamma_\sigma = \gamma_\sigma$ at renormalization scale μ . The

¹We employ Landau gauge and a Euclidean metric, with $\{\gamma_\mu, \gamma_\nu\} = 2\delta_{\mu\nu}$, $\gamma_\mu^\dagger = \gamma_\mu$, and $a \cdot b = \sum_{i=1}^4 a_i b_i$.

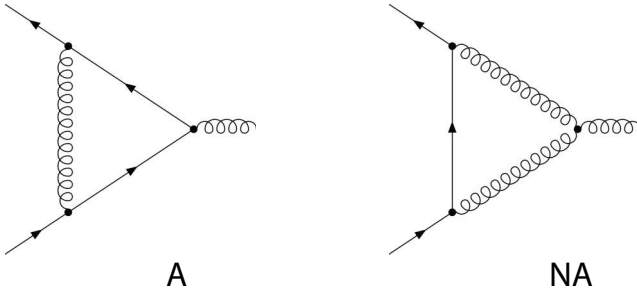


FIG. 1. The quark-gluon vertex at one loop. The left diagram labeled A is the Abelian-like term Γ_{σ}^A , and the right diagram labeled NA is the non-Abelian term $\Gamma_{\sigma}^{\text{NA}}$.

following quantities are bare: the three-gluon vertex $igf^{abc}\Gamma_{\mu\nu\sigma}^{3g}(q+k, q)$, the quark propagator $S_0(p)$, and the gluon propagator $D_{\mu\nu}(q) = T_{\mu\nu}(q)D_0(q^2)$, where $T_{\mu\nu}(q)$ is the transverse projector. The next order terms in Eq. (1) are $\mathcal{O}(g^3)$: the contribution involving the four-gluon vertex, and $\mathcal{O}(g^4)$: contributions from crossed-box and two-rung gluon ladder diagrams, and one-loop dressing of the triple-gluon vertex, etc.

The color factors in Eqs. (2) and (3), given by

$$\begin{aligned} t^a t^b t^a &= \left(C_F - \frac{C_A}{2}\right) t^b = -\frac{1}{2N_c} t^b, \\ t^a f^{abc} t^b &= \frac{C_A}{2} it^c = \frac{N_c}{2} it^c, \end{aligned} \quad (4)$$

reveal two important considerations. The color factor of the (Abelian-like) term Γ_{σ}^A would be given by $t^a t^a = C_F = (N_c^2 - 1)/2N_c$ for the strong dressing of the photon-quark vertex, i.e., in the color-singlet channel. The octet Γ_{σ}^A is of opposite sign and is suppressed by a factor $1/(N_c^2 - 1)$: Single gluon exchange between a quark and an antiquark has relatively weak repulsion in the color-octet channel, compared to strong attraction in the color-singlet channel. Net attraction for the gluon vertex (at least to this order) is provided by the non-Abelian $\Gamma_{\sigma}^{\text{NA}}$ term, which involves the three-gluon vertex: The color factor is amplified by $-N_c^2$ over the Γ_{σ}^A term.

The specific form of the bare triple-gluon vertex is conveniently expressed in terms of three momenta $p_1 = q + k$, $p_2 = -q$, and $p_3 = -k$, that are outgoing. Thus, with $\Gamma_{\mu\nu\sigma}^{3g}(q+k, q) \equiv \tilde{\Gamma}_{\mu\nu\sigma}^{3g}(p_1, p_2, p_3)$, we have

$$\begin{aligned} \tilde{\Gamma}_{\mu\nu\sigma}^{3g}(p_1, p_2, p_3) &= -\{(p_1 - p_2)_{\sigma} \delta_{\mu\nu} + (p_2 - p_3)_{\mu} \delta_{\nu\sigma} \\ &\quad + (p_3 - p_1)_{\nu} \delta_{\sigma\mu}\}, \end{aligned} \quad (5)$$

and the complete vertex is symmetric under permutations of all gluon coordinates. In Landau gauge $\Gamma_{\mu\nu\sigma}^{3g}$ obeys the Slavnov-Taylor identity

$$\begin{aligned} k_{\sigma} \Gamma_{\mu\nu\sigma}^{3g}(q+k, q) &= D_0^{-1}(q) T_{\mu\nu}(q) \\ &\quad - D_0^{-1}(q+k) T_{\mu\nu}(q+k). \end{aligned} \quad (6)$$

The nonperturbative model of Sec. III addresses the $k = 0$ case and makes an extension of the bare result

$$\Gamma_{\mu\nu\sigma}^{3g}(q, q) = -\frac{\partial}{\partial q_{\sigma}} D_0^{-1}(q) T_{\mu\nu}(q), \quad (7)$$

which allows the amplitude for the non-Abelian diagram at $k = 0$ to take the form

$$\begin{aligned} \Gamma_{\sigma}^{\text{NA}}(p, p) &= -i \frac{C_A}{2} \int_q^{\Lambda} \gamma_{\mu} S_0(p-q) \gamma_{\nu} \\ &\quad \times \left\{ \frac{\partial}{\partial q_{\sigma}} g^2 D_0(q^2) \right\} T_{\mu\nu}(q). \end{aligned} \quad (8)$$

It is easy to verify that the Abelian diagram gives

$$\Gamma_{\sigma}^A(p, p) = -i \left[1 - \frac{C_A}{2} C_F^{-1} \right] \frac{\partial}{\partial p_{\sigma}} \Sigma^{(1)}(p), \quad (9)$$

in terms of the one-loop self-energy.

The dressing provided by the combination $\Gamma_{\sigma}^A + \Gamma_{\sigma}^{\text{NA}}$ yields a vertex that satisfies the Slavnov-Taylor identity (STI) through $\mathcal{O}(g^2)$ [14]. This identity expresses the divergence of the vertex in terms of the bare and one-loop contributions to three objects: $S(p)^{-1}$, the ghost propagator dressing function, and the ghost-quark scattering amplitude. The one-loop $S(p)^{-1}$ part of this relation is generated partly from Γ_{σ}^A (with a weak repulsive color strength) and partly from $\Gamma_{\sigma}^{\text{NA}}$ (with the complementary strongly attractive color strength). The $\Gamma_{\sigma}^{\text{NA}}$ term also provides the explicitly non-Abelian terms of the $\mathcal{O}(g^2)$ STI.

III. NONPERTURBATIVE VERTEX MODEL

Our nonperturbative model for the dressed-quark-gluon vertex is defined by extensions of Eqs. (2) and (3) into dressed versions determined solely from an existing ladder-rainbow model DSE kernel. The bare quark propagators in Eqs. (2) and (3) are replaced by solutions of the quark DSE in rainbow truncation, namely,

$$\begin{aligned} S(p)^{-1} &= Z_2 i \not{p} + Z_4 m(\mu) \\ &\quad + C_F \int_{p'}^{\Lambda} \frac{\mathcal{G}(q^2)}{q^2} T_{\mu\nu}(q) \gamma_{\mu} S(p') \gamma_{\nu}, \end{aligned} \quad (10)$$

where $q = p - p'$. A particular ladder-rainbow kernel is specified by the effective quark-quark coupling $\mathcal{G}(q^2)$. Two different DSE models are employed and both have the ultraviolet behavior specified by QCD with one-loop renormalization group improvement, i.e., the one-loop renormalizations of the quark and gluon propagators and the pair of quark-gluon vertices have been absorbed so that $\mathcal{G}(q^2)$ matches $4\pi\alpha_s^{\text{one-loop}}(q^2) = 4\pi^2 \gamma_m / \ln(q^2/\Lambda_{\text{QCD}}^2)$ [15]. Here $\gamma_m = 12/(33 - 2N_f)$ is the anomalous mass dimension which arises in the leading logarithmic behavior of the quark mass function in the ultraviolet. The two DSE models differ in the infrared content of $\mathcal{G}(q^2)$ specified by parametrization.

The first model (DSE-Lat) [16] is defined by

$$\frac{\mathcal{G}(q^2)}{q^2} = D_{\text{lat}}(q^2)\Gamma_1[q^2, m(\mu)], \quad (11)$$

where $D_{\text{lat}}(q^2)$ is a fit to quenched-lattice data for the Landau gauge gluon propagator [17] that has the correct one-loop logarithmic behavior $\sim \ln(q^2/\Lambda_{\text{QCD}}^2)^{-13/22}$ in the ultraviolet. In the infrared $D_{\text{lat}}(q^2)$ is finite and is suppressed with respect to the bare propagator. The vertex factor $\gamma_\nu \Gamma_1[q^2, m(\mu)]$ represents the remaining one-loop renormalizations for ultraviolet matching to $4\pi\alpha_s^{\text{one-loop}}(q^2)/q^2$ (with $N_f = 0$) and also contains a parametrized representation of the remaining infrared dressing. Explicit formulas are given in Ref. [16]. Parameters are determined by requiring that the DSE solutions reproduce the quenched-lattice data [18] for $S(p)$ in the available domain $p^2 < 10 \text{ GeV}^2$ and $m(\mu = 2 \text{ GeV}) < 200 \text{ MeV}$. In this sense, the DSE-Lat model represents quenched dynamics. It is found that the necessary vertex dressing is a strong but finite enhancement. The model easily reproduces m_π with a current mass that is within acceptable limits. However, the resulting chiral condensate $\langle \bar{q}q \rangle_{\mu=1 \text{ GeV}}^0 = (0.19 \text{ GeV})^3$ is a factor of 2 smaller than the value $(0.24 \pm 0.01 \text{ GeV})^3$ from a best fit [19] of strong interaction observables [16]. This is attributed to the quenched approximation in the lattice data.

The second model (DSE-MT) [20] implements a one-parameter representation for the infrared sector of $\mathcal{G}(q^2)$ that is fit to the empirical chiral condensate. The explicit form is

$$\frac{\mathcal{G}(q^2)}{q^2} = \frac{4\pi^2 D q^2}{\omega^6} e^{-q^2/\omega^2} + \frac{4\pi^2 \gamma_m \mathcal{F}(q^2)}{\frac{1}{2} \ln[\tau + (1 + q^2/\Lambda_{\text{QCD}}^2)^2]}. \quad (12)$$

Here the first term implements the infrared enhancement necessary to generate the empirical condensate, while the second term, with $\mathcal{F}(s) = \{1 - \exp[-s/(4m_t^2)]\}/s$, connects smoothly with the one-loop renormalization group behavior of QCD. Apart from the fixed values $m_t = 0.5 \text{ GeV}$, $\tau = e^2 - 1$, $N_f = 4$, and $\Lambda_{\text{QCD}} = 0.234 \text{ GeV}$, the free parameters, ω and D , are not independent. The fitted observables are essentially constant along the trajectory $\omega D = (0.72 \text{ GeV})^3$ for $\omega = 0.3\text{--}0.5 \text{ GeV}$. A standard choice is $\omega = 0.4 \text{ GeV}$ and $D = 0.93 \text{ GeV}^2$. The model provides an excellent description of a wide variety of light-quark meson physics including the masses and decay constants of the light-quark pseudoscalar and vector mesons [15,20], the elastic charge form factors $F_\pi(Q^2)$ and $F_K(Q^2)$ [21], and the electroweak transition form factors of the pseudoscalars and vectors [22,23]. In this sense it represents unquenched dynamics.

In the ultraviolet, the $\bar{q}q$ scattering kernel appearing in the Abelian-like vertex diagram shown in Fig. 1(A) co-

incides with the ladder-rainbow kernel; thus the latter provides a suitable nonperturbative extension. We substitute $g^2 D_0(q^2) \rightarrow \mathcal{G}(q^2)/q^2$ in the integrand for Γ_σ^A in Eq. (2). The vertex for the external gluon is taken to be bare.

Even in the ultraviolet, the $\bar{q}q$ scattering kernel does not appear explicitly in the non-Abelian vertex diagram shown in Fig. 1(NA). However, at $k = 0$, the expression in Eq. (8) for $\Gamma_\sigma^{\text{NA}}(p, p)$ has combined the triple-gluon vertex and the gluon propagators to produce a form that emphasizes the close connection to the ladder kernel and the self-energy integral. The same nonperturbative extension $g^2 D_0(q^2) \rightarrow \mathcal{G}(q^2)/q^2$ now suggests itself for Fig. 1(NA), and we use it. Justifications for this choice are consistency and simplicity; no new parameters are introduced.

IV. RESULTS AND DISCUSSION

The general nonperturbative vertex at $k = 0$ has a representation in terms of three invariant amplitudes; here we choose

$$\Gamma_\sigma(p, p) = \gamma_\sigma \lambda_1(p^2) - 4p_\sigma \gamma \cdot p \lambda_2(p^2) - i2p_\sigma \lambda_3(p^2), \quad (13)$$

since the lattice-QCD data [12] is provided in terms of these $\lambda_i(p^2)$ amplitudes. A useful comparison is the corresponding vertex in an Abelian theory like QED; it is given by the Ward identity $\Gamma_\sigma^{\text{WI}}(p, p) = -i\partial S^{-1}(p)/\partial p_\sigma$ in terms of the exact propagator $S^{-1}(p)$. With $S^{-1}(p) = i\gamma \cdot p A(p^2) + B(p^2)$, this leads to the correspondence $\lambda_1^{\text{WI}} = A$, $\lambda_2^{\text{WI}} = -A'/2$, and $\lambda_3^{\text{WI}} = B'$, where $f' = \partial f(p^2)/\partial p^2$.

In Fig. 2 we display the DSE-Lat model results in a dimensionless form for comparison with the (quenched) lattice data.² The renormalization scale of the lattice data is $\mu = 2 \text{ GeV}$ where $\lambda_1(\mu) = 1$, $A(\mu) = 1$. We compare to the lattice data set for which $m(\mu) = 60 \text{ MeV}$. The same renormalization scale and conditions have been implemented for both DSE models.³ For λ_1 and λ_3 , we also compare with the Abelian *Ansatz* in which the amplitudes are obtained from the quark propagator through the Ward Identity, which is equivalent to the $k = 0$ limit of either the Ball-Chiu [6] or Curtis-Pennington [7] *Ansatz*. Without parameter adjustment, the model reproduces the lattice data for λ_1 and λ_3 quite well over the whole momentum range for which data is available. The Abelian *Ansatz*, while clearly inadequate for λ_1 below 1.5 GeV , reproduces λ_3 . The present lattice data for λ_2 has

²We note that in Ref. [12] both the lattice data and the Abelian (Ward identity) *Ansatz* for $\lambda_3(p)$ are presented as positive. These two sign errors have been acknowledged [13].

³To facilitate change of the scale μ , we have slightly modified both DSE kernels (both originally defined at fixed scale $\mu_0 = 19 \text{ GeV}$) by including the additional kernel strength factor $Z_2^2(\mu^2, \Lambda^2)/Z_2^2(\mu_0^2, \Lambda^2)$ recommended by Maris [24]. This does not alter results for observables.

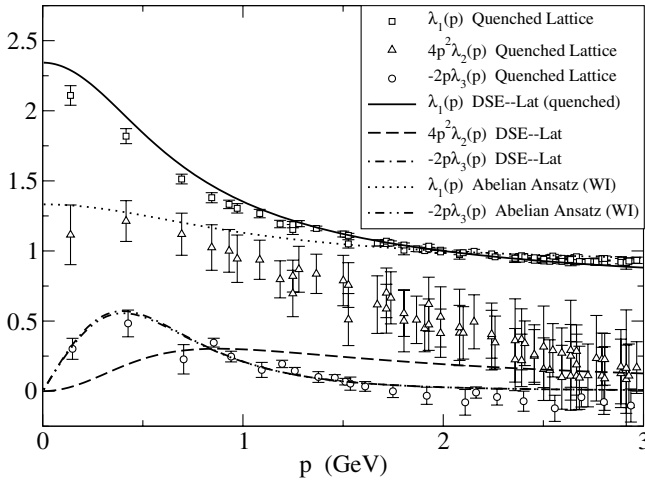


FIG. 2. The amplitudes of the dressed-quark-gluon vertex at zero gluon momentum and for quark current mass $m(\mu = 2 \text{ GeV}) = 60 \text{ MeV}$. Quenched-lattice data [12] is compared to the results of the DSE-Lat model [16]. The Abelian *Ansatz* (Ward identity) is also shown except for $\lambda_2(p)$ which is almost identical to the DSE-Lat model.

large errors; it suggests infrared strength that is seriously underestimated by the model. (The Abelian *Ansatz* for λ_2 is very close to the DSE model and, for reasons of clarity, is not displayed.)

The relative contributions to the vertex dressing made by $\Gamma_{\sigma}^{\text{NA}}$ and $\Gamma_{\sigma}^{\text{A}}$ are indicated by the following amplitude ratios at $p = 0$: $\lambda_1^{\text{NA}}/\lambda_1^{\text{A}} = -60$, $\lambda_2^{\text{NA}}/\lambda_2^{\text{A}} = -14$, and $\lambda_3^{\text{NA}}/\lambda_3^{\text{A}} = -12$. Thus, the non-Abelian term $\Gamma_{\sigma}^{\text{NA}}$ dominates to a greater extent than what the ratio of color factors (-9) would suggest; it also distributes its infrared strength to favor λ_1 more so than does $\Gamma_{\sigma}^{\text{A}}$. Since the momentum-dependent shapes of the $\lambda_i^{\text{NA}}(p)$ and $\lambda_i^{\text{A}}(p)$ are quite similar, the present model results could be summarized quite effectively by ignoring $\Gamma_{\sigma}^{\text{A}}$ and scaling $\Gamma_{\sigma}^{\text{NA}}$ up by about 10%.

Because of the definition of the two DSE models, their comparison in Fig. 3 provides an estimate of the effects of the quenched approximation. The effects are moderate within the present DSE model framework. Figure 3 also suggests that a model including the four-gluon vertex as well as the two diagrams of Fig. 1 should be considered, especially for amplitude λ_2 . The question of the importance of the iterations of the diagrams of Fig. 1 also arises. We have estimated such effects by iteration to all orders based on the ladder-rainbow kernel. This amounts to solution of a ladder Bethe-Salpeter integral equation in which the inhomogeneity is our dressed extension of $Z_{\text{IF}}\gamma_{\sigma} + \Gamma_{\sigma}^{\text{NA}}(p, p)$ and the kernel term is the dressed extension of $\Gamma_{\sigma}^{\text{A}}(p, p)$ with the internal γ_{σ} replaced by $\Gamma_{\sigma}(q, q)$. This generates very little change—significantly less than the quenching effect evident in Fig. 3. This is due to the small color factor of the kernel term. We have not

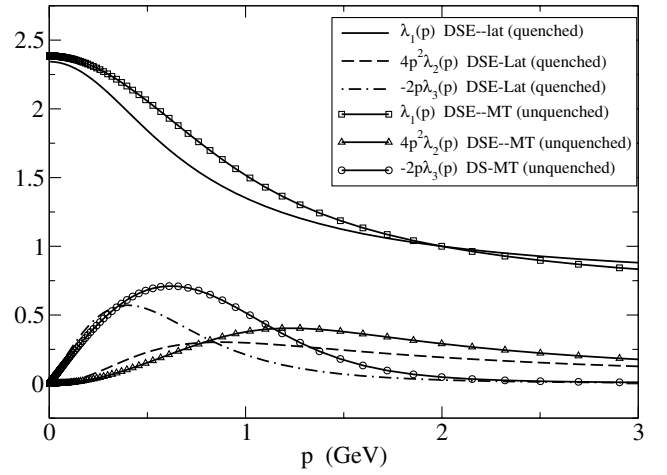


FIG. 3. The amplitudes of the dressed-quark-gluon vertex at zero gluon momentum, and for quark current mass $m(\mu = 2 \text{ GeV}) = 60 \text{ MeV}$, from two models: DSE-Lat [16] and DSE-MT [20] that relate to quenched and unquenched content, respectively.

explored the consequences of using the dressed vertex self-consistently for the internal quark-gluon vertices of $\Gamma_{\sigma}^{\text{NA}}$ in Fig. 1(NA).

The nonperturbative *Ansatz* we have applied to Eq. (8) for the non-Abelian diagram, Fig. 1(NA), effectively includes dressing of the triple-gluon vertex $\Gamma_{\mu\nu\sigma}^3$. Some perturbative studies of $\Gamma_{\mu\nu\sigma}^3$ have been made at one loop [25,26] but they provide no guidance for extension to infrared scales. The nonperturbative *Ansätze* for $\Gamma_{\mu\nu\sigma}^3$ suggested in Refs. [2,27] for use within truncated gluon-ghost-quark DSEs require explicit models for the ghost dressing function and the ghost-gluon vertex that appear in the STI for $\Gamma_{\mu\nu\sigma}^3$. Such considerations are beyond the scope of the present work; they would entail additional parameters that are not warranted at this stage.

A different approach to the nonperturbative extension of the non-Abelian diagram, Fig. 1(NA), has recently been explored in Refs. [10,11]. That approach employs a bare triple-gluon vertex and dressed gluon two-point functions resulting from previous solution of a truncation of the coupled ghost-gluon-quark DSEs [3]. (The quark-gluon vertex within that calculation was described by the Curtis-Pennington [7] Abelian *Ansatz* times the square of the infrared enhanced ghost dressing function.) The strong infrared suppression inherent in such gluon propagator solutions produces a very weak quark-gluon vertex unless the internal quark-gluon vertices of Fig. 1(NA) are also enhanced. References [10,11] proceed by assuming that attachment of a single ghost dressing function to each vertex is appropriate for this. The results are similar to the present work, except that the $m(\mu) = 115 \text{ MeV}$ case is considered [10,11].

The infrared content of QCD two-point and three-point functions is not a settled subject and there is much to be gained from comparison of a variety of modeling strategies. Our approach to the vertex differs from Refs. [10,11] in the following respect. We exploit the similarity between Eq. (8) for $\Gamma_{\sigma}^{\text{NA}}(p, p)$ and a zero momentum gluon insertion into the lowest order $\bar{q}q$ scattering kernel appearing in the rainbow diagram for the quark self-energy. Note that if the derivative in Eq. (8) were to act also on the transverse projector, the result would be an Abelian-like derivative of the self-energy. The correction terms to this are evidently small for the resulting amplitudes λ_2 and λ_3 , but they are large for λ_1 . Since the renormalization group improved DSE-Lat kernel has infrared content that supplements quenched-lattice data for the gluon two-point function to get a precise fit to the quenched-lattice quark propagator mass function, it is not surprising that our result for λ_3 is a closer representation of the lattice data than the corresponding result from Refs. [10,11]. The latter works do not determine parameters by fitting the quark propagator.

Our approach induces effective dressing of the gluon propagators, internal quark vertices, and the triple-gluon vertex in one quantity that is tightly constrained by quenched-lattice data for two-point functions. There is no well-defined and consistent way to separate the various contributions. If we assume this $\bar{q}q$ kernel can be used for each quark-gluon interaction in Fig. 1(NA) then our *Ansatz* is equivalent to corresponding use of a dressed triple-gluon vertex $\Gamma_{\mu\nu\sigma}^{3g}$ satisfying Eqs. (6) and (7) with the substitution $D_0(q^2) \rightarrow [\mathcal{G}(q^2)/g^2(\mu^2)]/q^2$. If one were to replace this by the bare vertex, leaving other factors unchanged, then the final vertex amplitudes in-

crease by at least an order of magnitude; the infrared dressing enhancements have been treated inconsistently. An opposite extreme, that is at least consistent, is to use the bare limit for all elements of Fig. 1(NA) except for the quark propagator. That is, use $D_0(q^2) \rightarrow 1/q^2$ in Eq. (8). This underestimates the quark-gluon vertex amplitudes by an order of magnitude. In the absence of clear guidance for the infrared content of each of the two-point and three-point functions involved, the consistent use of an empirical ladder-rainbow kernel representation of the $\bar{q}q$ scattering amplitude recommends itself.

An issue of consistency that requires future attention is the following. Both lattice data and the present model calculation indicate that vertex amplitude λ_1 is infrared enhanced to about 2.5 times the bare value. However, the phenomenological vertex enhancement found in the DSE-Lat model (assumed to be concentrated solely in that single amplitude) is about 6 times this at a typical infrared point $p^2 \sim 0.04 \text{ GeV}^2$ [28]. The proper distribution of vertex strength over the many amplitudes available at finite momenta may be part of the resolution. On a more general note, it would be desirable to replace the phenomenological aspects of the dressing effects implicitly included for the internal quark-gluon vertices by the results of explicit model calculations.

ACKNOWLEDGMENTS

The authors would like to thank R. Alkofer, C. D. Roberts, A. Kızılersü, J. I. Skullerud, and M. A. Pichowsky for useful discussions. We are grateful to J. I. Skullerud for providing the lattice-QCD results. This work has been partially supported by NSF Grants No. PHY-0301190 and No. INT-0129236.

-
- [1] P. Maris and C. D. Roberts, *Int. J. Mod. Phys. E* **12**, 297 (2003).
 - [2] R. Alkofer and L. von Smekal, *Phys. Rep.* **353**, 281 (2001).
 - [3] C. S. Fischer and R. Alkofer, *Phys. Rev. D* **67**, 094020 (2003).
 - [4] M. S. Bhagwat, A. Holl, A. Krassnigg, C. D. Roberts, and P. C. Tandy, *Phys. Rev. C* **70**, 035205 (2004).
 - [5] P. Watson, W. Cassing, and P. C. Tandy, hep-ph/0406340.
 - [6] J. S. Ball and T.-W. Chiu, *Phys. Rev. D* **22**, 2542 (1980).
 - [7] D. C. Curtis and M. R. Pennington, *Phys. Rev. D* **42**, 4165 (1990).
 - [8] P. Maris, C. D. Roberts, and P. C. Tandy, *Phys. Lett. B* **420**, 267 (1998).
 - [9] A. Bender, C. D. Roberts, and L. Von Smekal, *Phys. Lett. B* **380**, 7 (1996).
 - [10] C. S. Fischer, F. Llanes-Estrada, and R. Alkofer, hep-ph/0407294.
 - [11] F. J. Llanes-Estrada, C. S. Fischer, and R. Alkofer, hep-ph/0407332.
 - [12] J. I. Skullerud, P. O. Bowman, A. Kızılersü, D. B. Leinweber, and A. G. Williams, *J. High Energy Phys.* **04** (2003) 047.
 - [13] J.-I. Skullerud, P. O. Bowman, A. Kızılersü, D. B. Leinweber, and A. G. Williams, hep-lat/0408032.
 - [14] A. I. Davydychev, P. Osland, and L. Saks, *Phys. Rev. D* **63**, 014022 (2001).
 - [15] P. Maris and C. D. Roberts, *Phys. Rev. C* **56**, 3369 (1997).
 - [16] M. S. Bhagwat, M. A. Pichowsky, C. D. Roberts, and P. C. Tandy, *Phys. Rev. C* **68**, 015203 (2003).
 - [17] UKQCD Collaboration, D. B. Leinweber *et al.*, *Phys. Rev. D* **60**, 094507 (1999).
 - [18] P. O. Bowman, U. M. Heller, D. B. Leinweber, and A. G. Williams, *Nucl. Phys., Proc. Suppl.* **119**, 323 (2003).
 - [19] D. B. Leinweber, *Ann. Phys. (N.Y.)* **254**, 328 (1997).
 - [20] P. Maris and P. C. Tandy, *Phys. Rev. C* **60**, 055214 (1999).

- [21] P. Maris and P.C. Tandy, Phys. Rev. C **62**, 055204 (2000).
- [22] P. Maris and P.C. Tandy, Phys. Rev. C **65**, 045211 (2002).
- [23] C.-R. Ji and P. Maris, Phys. Rev. D **64**, 014032 (2001).
- [24] P. Maris (private communication).
- [25] A. I. Davydychev, P. Osland, and O.V. Tarasov, Phys. Rev. D **54**, 4087 (1996); **59**, 109901(E) (1999).
- [26] A. I. Davydychev, P. Osland, and L. Saks, J. High Energy Phys. 08 (2001) 050.
- [27] C. S. Fischer, R. Alkofer, and H. Reinhardt, Phys. Rev. D **65**, 094008 (2002).
- [28] P.C. Tandy, nucl-th/0408037.